Korean J. Chem. Eng., **31**(4), 630-638 (2014)
DOI: 10.1007/s11814-013-0285-3

pISSN: 0256-1115
eISSN: 1975-7220

Reductive removal of hexavalent chromium from aqueous solution using sepiolite-stabilized zero-valent iron nanoparticles: Process optimization and kinetic studies

Amirhosein Ramazanpour Esfahani*,†, Saeid Hojati*, Amin Azimi, Leila Alidokht***, Alireza Khataee****,†, and Meysam Farzadian***

*Department of Soil Science, Faculty of Agriculture, Shahid Chamran University, Ahvaz, Iran
**Department of Soil Science, Faculty of Agriculture,
Islamic Azad University of Science and Research of Khorasgan, Esfahan, Iran
***Department of Soil Science, Faculty of Agriculture, University of Tabriz, Tabriz, Iran
****Research Laboratory of Advanced Water and Wastewater Treatment Processes,
Department of Applied Chemistry, Faculty of Chemistry, University of Tabriz, Tabriz, Iran
(*Received 22 September 2013 • accepted 18 December 2013*)

Abstract−We studied the optimization of hexavalent chromium (Cr(VI)) removal from aqueous solution using the synthesized zero-valent iron nanoparticles stabilized with sepiolite clay (S-ZVIN), under various parameters such as reaction time (min), initial solution pH and concentration of S-ZVIN ($g \cdot L^{-1}$) using response surface methodology (RSM). The kinetic study of Cr(VI) was conducted using three types of the most commonly used kinetic models including pseudo zero-order, pseudo first-order, and pseudo second-order models. The rate of reduction reaction showed the best fit with the pseudo first-order kinetic model. The process optimization results revealed a high agreement between the experimental and the predicted data (R^2=0.945, Adj-R^2=0.890). The results of statistical analyses showed that reaction time was the most impressive factor influencing the efficiency of removal process. The optimum conditions for maximum response (98.15%) were achieved at the initial pH of 4.7, S-ZVIN concentration of 1.3 $g \cdot L^{-1}$ and the reaction time of 75 min.

Keywords: Zero-valent Iron, Sepiolite, Hexavalent Chromium, Response Surface Methodology, Central Composite Design

INTRODUCTION

Chromium is a transition-group metal with oxidation states ranging from −2 to +6, of which the trivalent and hexavalent forms are the most stable states in the environment [1]. The maximum permissible level of Cr(VI) in drinking water has already been specified as 0.05 $mg \cdot L^{-1}$ by the World Health Organization [2]. High levels of Cr(VI) compounds in the environment are mostly caused by industrial activities including pigment manufacturing, stainless steel production, leather tanning, metal finishing, and chrome plating. followed by lack of proper disposal facilities [3]. Hexavalent chromium (VI) compounds are known to be human carcinogens and mutagens, whereas trivalent chromium (Cr(III)) compounds are less toxic, non-carcinogenic and less mobile due to precipitation as chromium hydroxides or adsorption onto the mineral surfaces [4]. Therefore, reducing Cr(VI) to Cr(III) might be a feasible and environmentally beneficial approach for remediation of Cr(VI)-contaminated sites. The potential limitation of this approach is the re-oxidation of the reduced Cr(III) to Cr(VI) in the presence of MnO_2 as a powerful oxidizer in the environment. This limitation can be overcome by using Fe-bearing reductants such as Fe(0) and Fe(II), where reduced Cr(III) ultimately precipitates as mixed Fe(III) - Cr(III) hydroxide/oxyhydroxide [1,5,6].

Recently, application of zero-valent iron nanoparticles with high surface area and reductive characteristics has been suggested as a promising technique for the removal of several environmental pollutants. A large number of hazardous contaminants such as nitrate [7], Cr(VI) [8,9], Pb^{2+} [10], polychlorinated biphenyls [11,12], nitroaromatic compounds [13,14], and chlorinated pesticides [15] can be removed successfully using ZVIN. ZVIN can be synthesized through the reduction of dissolved iron by means of sodium or potassium borohydride [16]. However, the chemical synthesis of ZVIN is not completely a flawless process.

Generally, the bare or uncoated ZVINs, like other nanoparticles, are prone to agglomerate in aqueous media and create large particles with micro or millimeter diameters which lead to decreasing the reactivity of the particles toward target pollutant. The reason for particle agglomeration is related to the magnetic attraction forces between the particles [17]. Recently, several stabilizers namely, carboxymethyl cellulose (CMC) [18], polyacrylic acid (PAA) [19], guar gum [20], and starch [21] have been used to enhance the colloidal stability as well as the surface area of ZVIN. Although these stabilizers represent perfect performance by way of enhancing the stabilization of ZVIN, natural stabilizers have replaced them due to their costs and environmental hazards.

Recently, the inclination to use porous materials to stabilize ZVIN has been observed in some researches. Zhang et al. [22] reported that kaolinite is as an ideal stabilizer of ZVIN to treat Pb^{2+}-contaminated solutions [22]. Besides, sepiolite is not only an abundant clay mineral in arid and semi-arid regions of the world, but is also cost-

†To whom correspondence should be addressed.
E-mail: ramazanpour67@gmail.com, a_khataee@tabrizu.ac.ir

effective and environmentally friendly with no poisonous effects on the environment. Therefore, it is a good option to be used as stabilizing agent for ZVIN.

We used experimental design methodology to investigate the influence of three experimental parameters (initial solution pH, S-ZVIN concentration and reaction time) on the efficiency of the reductive removal of Cr(VI), and then to determine the optimal removal conditions. In most treatment processes, the statistical model that relates some controllable variables and their interaction effects to a response is quite complex, and the conventional methods used to determine this relationship are time-consuming, work demanding and costly. In this respect, experimental designs such as central composite design (CCD), as the most popular design in RSM, are appropriate tools to overcome these limitations and to find improved or optimal process conditions to use the resources efficiently.

Response surface methodology has been applied to model and optimize several wastewater treatment processes including photocatalysis [23,24], biosorption [25,26], electrochemical oxidation [27,28], adsorption [29], photoelectro-Fenton [30] and reduction [10]. Alidokht et al. [31] have reported that RSM can be successfully applied for the optimization of Cr(VI) removal process using starch-stabilized ZVIN in a Cr-spiked soil [31].

The aim of the present research was to optimize the process of Cr(VI) removal from aqueous solutions using the synthesized zero-valent iron nanoparticles stabilized with sepiolite at different experimental variables, including initial pH of the aqueous solution, reaction time (min) and concentration of S-ZVIN ($g \cdot L^{-1}$). In addition, an attempt was made to find the best kinetic model among the most commonly used ones.

EXPERIMENTAL

1. Materials

Ferrous sulfate heptahydrate ($FeSO_4 \cdot 7H_2O$) was purchased from AppliChem Co. Sodium borohydride (>98.5%), concentrated hydrochloric acid, sodium hydroxide, acetone, potassium dichromate ($K_2Cr_2O_7$) and 1, 5 diphenylcarbazide were purchased from Merck. Sepiolite clay was provided by DaneshBonyadFarapouyanIsatis Co, Yazd, Iran. Prior to use, it was ground using a ball mill and then passed through a 0.053 mm sieve.

2. Instrumentation

A scanning electron microscope (SEM) (Hitachi, S 4160, Japan) was used to determine the size and morphology of synthesized ZVIN. A 0.1 $g \cdot L^{-1}$ of S-ZVIN suspension was prepared for ultrasound experimentation using a DSA100-SK2 (South Korea) ultrasonic instrument for 15 min. Next, a drop of the suspension was placed on the plate and then put into the SEM instrument. A LEO 906E transmission electron microscope (TEM) was applied to prepare a TEM image of sepiolite for the determination of its particles size. An energy dispersive X-ray spectroscope (EDS) installed on SEM was used to analyze the elemental compositions of sepiolite and S-ZVIN. Finally, a UV-visible spectrophotometer (Unico, Spain) with 200-1,000 nm wavelength range was used to measure the concentration of Cr(VI) in residual solution in the wavelength of 540 nm.

3. Synthesis of Sepiolite-stabilized ZVIN (S-ZVIN)

The synthesis procedure of S-ZVIN was based on the reduction of ferrous sulfate using sodium borohydride in conjunction with sepiolite as stabilizer. First, 100 mL of 0.065 M ferrous sulfate solution (0.065 M $FeSO_4$) was added to 100 mL of distilled water containing 1 g of sepiolite using magnetic stirrer for 30 min (Heidolph, Germany). Afterwards, 20 mL of 1.05 M sodium borohydride solution (1.05 M $NaBH_4$) was added to the mixture using dropping funnel in a constant rate of 3 mL per minute so that extremely tiny black particles were produced. The produced particles were separated from the solution with a strong magnet and then kept in desiccator under vacuum for 24 hours to be dried. All synthesis procedures of S-ZVIN were performed under N_2 atmosphere to prevent oxidation of ZVIN.

4. Batch Experiments for Cr(VI) Removal

Batch experiments were performed in plastic bottles involving 100 $mg \cdot L^{-1}$ of Cr(VI) and in the presence of different concentrations of S-ZVIN (0.5, 0.75, 1.0, 1.5 and 2 $g \cdot L^{-1}$), different initial pH values (3, 6 and 9) and different reaction times (5-90 min). The initial pH of solutions was set using 0.1 M NaOH and 0.1 M HCl. During the experiment, tubes were shaken by a reciprocal shaker at 120 rpm. Then, after completion of the reaction, the tubes were centrifuged at 5,000 rpm for 5 min. The reacted S-ZVIN was then filtered using Whatman No. 42 filter paper and the residual solution was prepared to determine its Cr(VI) concentration. The diphenylcarbazide colorimetric method was employed to determine the residual concentration of the Cr(VI) and the removal efficiency (%) of Cr(VI) was calculated through the following equation [32]:

$$\text{Cr(VI) removal efficiency } (\%) = \frac{C_0 - C}{C_0} \times 100 \quad (1)$$

where C_0 and C are the initial and residual concentrations of Cr(VI), respectively.

5. Experimental Design

Response surface methodology was applied for optimizing the contaminant treatment process. In this study, central composite design (CCD) was employed for the optimization of operational conditions in removal efficiency of Cr(VI) from aqueous solution using S-ZVIN. To examine the removal efficiency of Cr(VI), three independent variables including pH of the aqueous solution, S-ZVIN concentration ($g \cdot L^{-1}$) and reaction time (min) were chosen.

The equation below was applied to obtain the total number of experiments (N):

$$N = 2^k + 2k + C_0 \quad (2)$$

where k is the number of factors, 2^k represents the number of factorial points, 2k is the number of axial points, and C_0 is the central points (in this study, were respectively 8, 6 and 6).

From the point of statistical calculation, each variable (X_i) was coded as x_i based on the following equation:

$$x_i = \frac{X_i - X_0}{\delta X} \quad (3)$$

Table 1. The natural values of independent factors

Variable	Range and level				
	1.682	1	0	−1	−1.682
Reaction time (min)	95	77	50	23	5
pH	9.5	8.08	6	3.92	2.5
S-ZVIN concentration ($g \cdot L^{-1}$)	2	1.65	1.13	0.6	0.25

where X_0 is the central point value of X_i and δX is the step change [33,34]. The natural values of each independent variable are given in Table 1.

6. Statistical Analysis

To correlate the dependent and independent parameters in the present study, a second-order polynomial model was applied as follows:

$$y = b_0 \sum b_i x_i + \sum b_{ii} x_i^2 + \sum b_{ij} x_i + x_j + \varepsilon \quad (4)$$

where y is the response variable of Cr(VI) removal efficiency, b_0 is the constant and b_i is the linear effect of factor x_i (i=1, 2 and 3). In addition, b_{ii} is the regression coefficient for the quadratic effect of factor x_i, b_{ij} is defined as an interaction effect between two factors of x_i and x_j (i=1, 2 and 3; j=1, 2 and 3) and finally, ε is the residual term.

The results of the CCD experiments were analyzed by using the software Design-Expert (version 8.0.0). Analysis of variance (ANOVA) was required to test the significance and adequacy of the model. Fisher's test (F-test), R^2, the adjusted-R^2 as ANOVA as well as the residuals analysis were chosen as model evaluation tools. The model coefficients were estimated using the least squares regression technique and the statistical significance (at the 95% confidence level) of the obtained model and the regression coefficients were evaluated using Fisher's variance analysis (F-test).

The model F-value is equal to the ratio between the mean square of the model and the residual error. If the model is statistically significant and therefore appropriate to predict the experimental responses, the model F-value should be greater than the tabulated value of F in specific domains of the degree of freedom at a significance level of α.

R^2 is a key factor which was applied to describe quantitatively the mutual relationship between the experimental and predicted values. Furthermore, fitness of the model was examined using the residuals (differences between experimental and predicted responses).

To evaluate the influence of each variable as well as their interaction effects on Cr(VI) removal efficiency, Pareto analysis was done using the following equation [35]:

$$p_i = \left(\frac{b_i^2}{\sum b_i^w} \right) \times 100, \ (i \neq 0) \quad (5)$$

where b is the regression coefficient of each parameter.

The two-dimensional contour plots and the three-dimensional surface plots were depicted using Design-Expert software.

7. Kinetic Studies

To arrive at a better description of the process of Cr(VI) removal, three kinetic models, pseudo zero-order, pseudo first-order and pseudo second-order, were evaluated. Eq. (6) represents the pseudo zero-order kinetic model [36]:

$$C_0 - C = k_{zero} t \quad (6)$$

where k_{zero} is the pseudo zero-order rate constant, t is the reaction time (min), and C and C_0 represent the residual and initial Cr(VI) concentrations ($mg \cdot L^{-1}$), respectively. k_{zero} can be obtained from the slope of the linear plot of $C_0 - C$ versus t at different pH values and S-ZVIN concentrations ($g \cdot L^{-1}$).

The pseudo first-order kinetic model, which is the most common model in wastewater treatment kinetic studies, is expressed as follows [37]:

$$\ln\left(\frac{C}{C_0}\right) = k_{obs} t \quad (7)$$

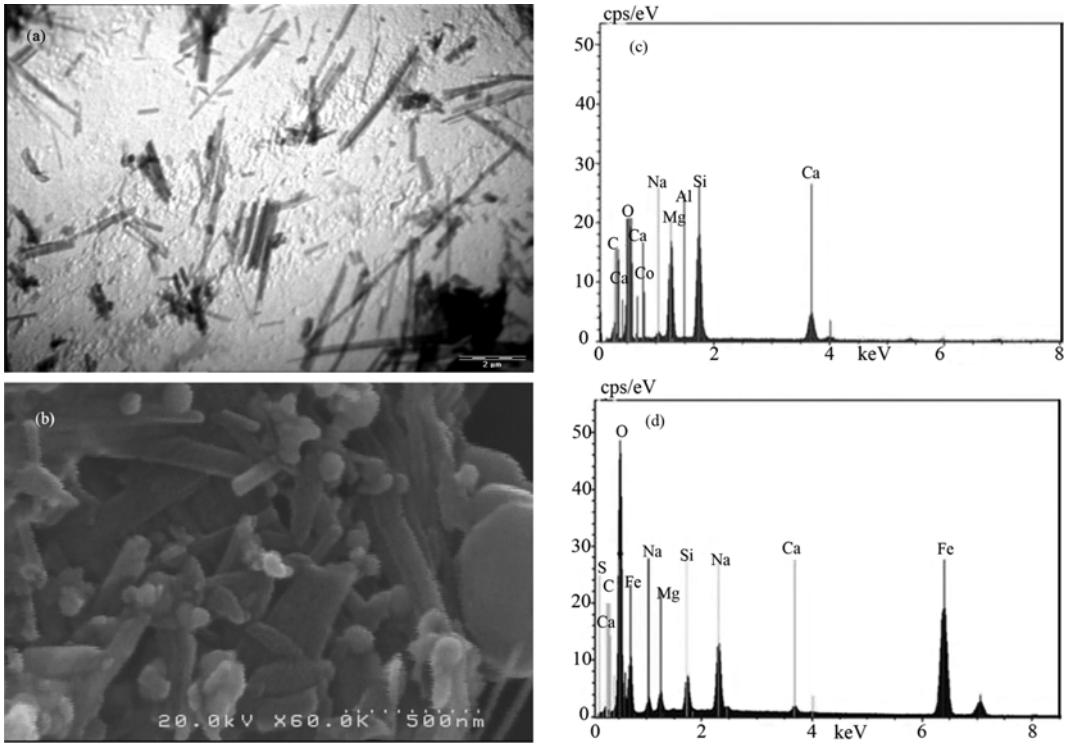

Fig. 1. (a) TEM image of sepiolite, (b) SEM image of S-ZVIN, (c) EDS spectrum of sepiolite and (d) EDS spectrum of S-ZVIN.

where k_{obs} is the pseudo first-order rate constant. The terms C, C_0 and t are described previously.

Finally, the pseudo second-order kinetic model is based on the following equation (Eq. (8)):

$$1/C=kt+1/C_0 \quad (8)$$

where k represents the pseudo second-order rate constant, obtained from the slope of the linear plot of 1/C against t. Other parameters in this equation have the same definitions as in Eq. (6).

RESULTS AND DISCUSSION

1. Characteristics of Synthesized S-ZVIN

A transmission electron micrograph of sepiolite is shown in Fig. 1(a). From Fig. 1(a), the needle-like shape of sepiolite with an average size of 1.6 micrometer was observed. Fig. 1(b) represents the SEM image of S-ZVIN. As can be seen, stabilized-ZVIN has a mixed shape in which spheroidal Fe particles with average diameters less than 100 nm are jointed with sepiolite. In addition, the EDS analysis of sepiolite and S-ZVIN is illustrated in Fig. 1(c) and (d), respectively. As seen in Fig. 1(c), the presence of sepiolite is supported by sharp peaks of O, Si and Mg and a weak peak that shows a small amount of Al in the structure of sepiolite. The occurrence of Ca could be related to the impurity of carbonates [38]. The EDS analysis of S-ZVIN (Fig. 1(d)) shows an additional sharp peak of Fe that implies joining of Fe^0 nanoparticles with sepiolite. Furthermore, Na and S peaks are thought to have originated from ferrous sulfate and sodium borohydride used for the synthesis of ZVIN particles.

2. Model Results for Reductive Removal of Cr(VI)

The statistical results between the response and independent variables were expressed using the second-order polynomial equation (Eq. (9)) as follows:

$$y=86.14+7.68X_1-8.15X_2+10.15X_3+0.48X_1X_2-1.66X_1X_3 -0.38X_2X_3-4.77X_1^2-2.69X_2^2-3.6X_3^2 \quad (9)$$

subject to $-1.682<x_i<+1.682$.

The 3-factor central composite design matrix and the experimental and predicted responses for Cr(VI) removal efficiencies are presented in Table 2. To ensure the adequacy of the model, the coefficient of determination (R^2) can be a handy tool. The obtained R^2 value of the model was high (R^2=0.945, Adj-R^2=0.890), implying that 94.5% of the variations for Cr(VI) removal efficiency are explained by the independent variables and only about 5.5% of variation cannot be explained by the model. The relationship between the experimental and predicted values for Cr(VI) removal was established. High R^2 value (0.945) indicated that the experimental values match well with the predicted values.

Table 2. The three independent factors and the value of dependent response (%)

Run order	S-ZVIN concentration ($g \cdot L^{-1}$)	pH	Reaction time (min)	Cr (VI) removal	
				Experimental (%)	Predicted (%)
1	1.65	8.08	23	68.54	66.97
2	1.13	6.00	50	85.33	86.14
3	1.13	6.00	50	86.90	86.14
4	0.60	8.08	77	74.69	70.20
5	0.60	3.92	23	67.71	63.85
6	1.13	6.00	95	91.69	93.00
7	1.65	8.08	77	83.45	83.20
8	1.13	6.00	50	87.42	86.14
9	1.13	6.00	50	85.44	86.14
10	1.13	9.50	50	59.57	64.84
11	1.65	3.92	77	97.53	99.29
12	0.60	8.08	23	53.21	47.34
13	1.13	6.00	5	54.36	58.87
14	1.13	2.50	50	91.69	92.24
15	1.13	6.00	50	88.56	86.14
16	1.13	6.00	50	84.18	86.14
17	0.60	3.92	77	90.75	88.21
18	2.00	6.00	50	87.73	85.56
19	1.65	3.92	23	81.16	81.54
20	0.25	6.00	50	51.75	59.74

The ANOVA results are presented in Table 3. Accordingly, the calculated F-value (19.10) was apparently greater than the tabulated-F (4.95), which clearly approves the significance of the model fits at a confidence level of 95%. Furthermore, residuals versus predicted responses are plotted as given in Fig. 2. This plot shows the residuals versus the ascending predicted response values, serving to test the assumption of constant variance. The plot should be a random scatter with a constant range of residuals across the graph. Fig. 2(b) illustrates that the residuals in the plot fluctuate in a random pattern around the central line.

Regression coefficients along with F-values and corresponding P-values are given in Table 4. The P-values are used to check whether the value of F is large enough to indicate statistical significance of the coefficient. Coefficients with P-values lower than 0.05 are significant at the confidence level of 95%. [39]. Furthermore, according to Pareto analysis, among all parameters, the linear effects of reaction time (b_3: 37.52%), initial pH of solution (b_2: 24.19%) and S-ZVIN concentration (b_1: 21.48%) were the most prominent factors in Cr(VI) removal process using S-ZVIN, respectively.

Table 3. The analysis of variance (ANOVA) of the experimental results of CCD

Variation sources	Sum of squares	Degree of freedom	Adjusted mean square	F-value
Regressions	3668.26	9	407.58	19.10
Residuals	213.44	10		
Total	3881.70	19		

R^2=0.945, Adj-R^2=0.890

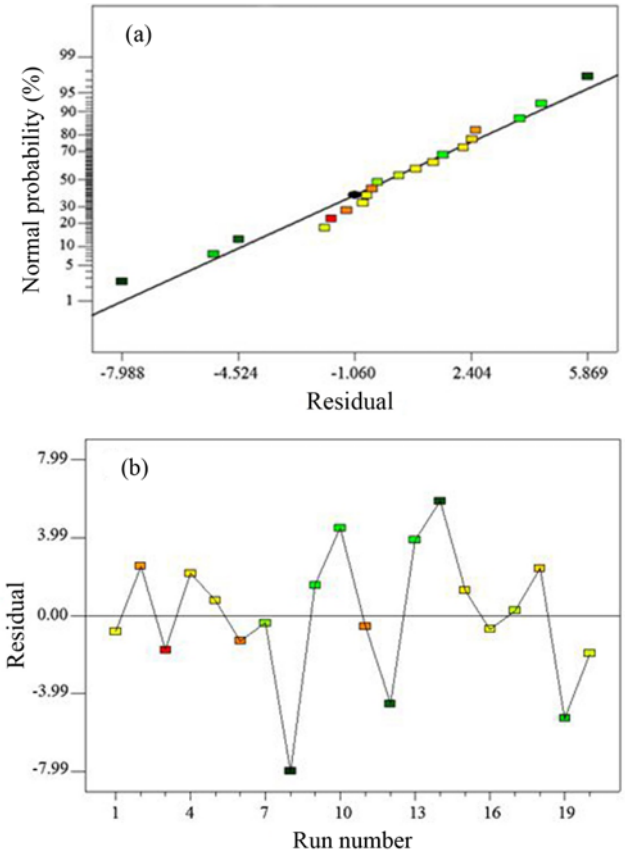

Fig. 2. Residual plots for Cr(VI) removal efficiency.

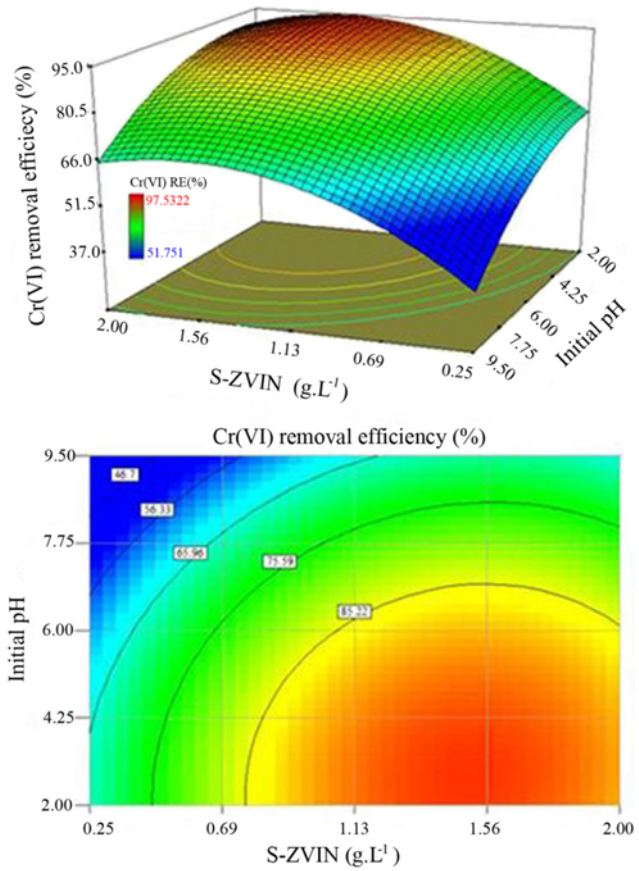

Fig. 3. The response surface and contour plot of Cr(VI) removal as a function of pH of aqueous solution and S-ZVIN dosage (g·L^{-1}).

Table 4. The obtained regression coefficients corresponding to the model based on experimental variables

Coefficients	Parameter estimate	F-value	P-value
b_0	86.14	19.1	<0.0001
b_1	7.68	37.7	0.0001
b_2	−8.15	42.48	<0.0001
b_3	10.15	65.9	<0.0001
b_{12}	0.48	0.087	0.7738
b_{13}	−1.66	1.03	0.3347
b_{23}	−0.38	0.054	0.8216
b_{11}	−4.77	15.36	0.0029
b_{22}	−2.69	4.87	0.0518
b_{33}	−3.6	8.79	0.0518

3. Effect of Variables on Cr(VI) Removal Efficiency

The contour and surface plots play important role in elaborating the systems with multiple variables and outputs. The contour plots of each variable against the rest of the experimental factors demonstrate how a certain variable has a relationship with another factor in a constant value of a third variable. In all of the experiments, one factor was kept constant while the two others were changed. Figs. (3-5) represent the contour and surface plots of Cr(VI) removal efficiency under different experimental conditions, namely the pH of aqueous solution, reaction time (min), and S-ZVIN concentration (g·L^{-1}). Fig. 3 shows the interaction impact of the initial solution pH and S-ZVIN concentration at constant reaction time on the removal efficiency of Cr(VI) in 100 mg·L^{-1} solution. As can be seen, the Cr(VI) removal efficiency has an inverse relationship with an increase of pH value, but a direct correlation with the concentration of S-ZVIN. It is clear that at low pH values, the removal efficiency of Cr(VI) increased to 97.53%. However, at higher pH values, it decreased to about 51%. The most plausible explanation is that in low pH values, the surface corrosion of zero-valent, due to the abundance of proton (H^+), led to enhancing the removal efficiency of Cr(VI) [40]. However, at alkaline pH, an increase of hydroxyl groups (OH^-) brought about an oxide layer and precipitated Cr(VI) layer onto the surfaces of zero-valent iron nanoparticles, which prevented corrosion of ZVIN surfaces and consequently reduced the removal rate of Cr(VI) [41-43]. Similarly, Alidokht et al. [8] reported that removal efficiency of Cr(VI) was remarkably decreased by increasing pH from 3 to 9 [8].

Fig. 4 shows the combined effect of reaction time and pH of an aqueous solution on the removal efficiency of 100 mg·L^{-1} Cr(VI) solution. At high reaction times and low pH values, removal efficiency hits its maximum values, so it is obvious that at the primary steps of reaction, the electron transfer from S-ZVIN to Cr(VI) was high. However, as the time passes, the rate of Cr(VI) removal reaction is slightly decreased. It can be stated that a significant decrease in the Cr(VI) removal efficiency was related to the creation of passivated film on the surfaces of ZVIN, leading to the loss of ZVIN reactivity with Cr(VI) [44].

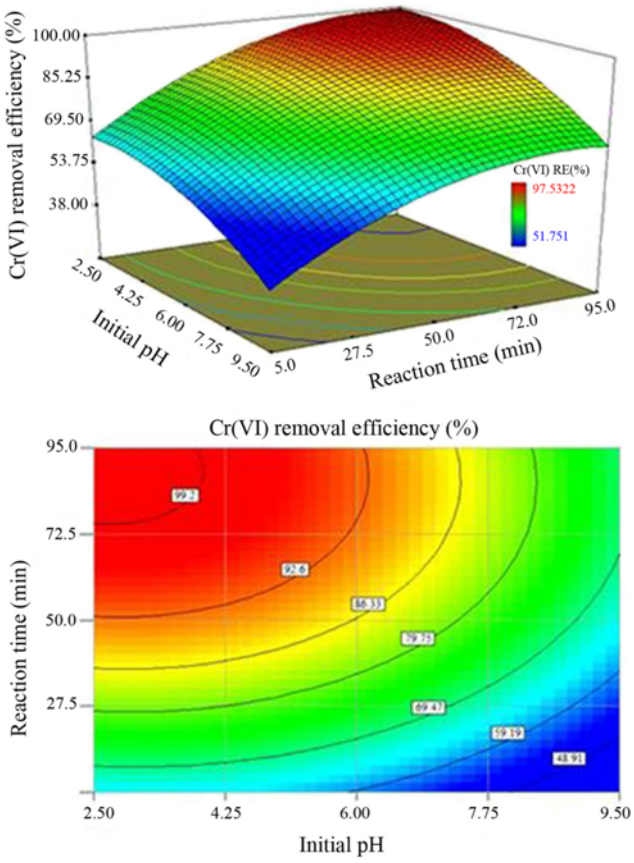

Fig. 4. The response surface and contour plot of Cr(VI) removal as a function of reaction time (min) and pH of aqueous solution.

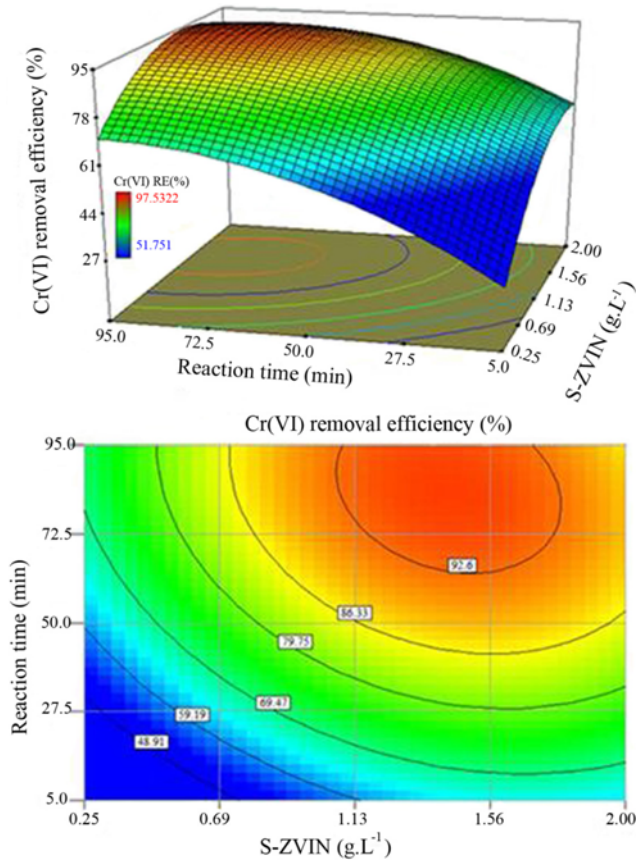

Fig. 5. The response surface and contour plot of Cr(VI) removal as a function of reaction time (min) and S-ZVIN dosage (g·L^{-1}).

The integrated influence of the reaction time and S-ZVIN concentration on Cr(VI) removal efficiency was evaluated at initial pH of 6 and results are shown in Fig. 5. The results demonstrate that much higher removal efficiency of Cr(VI) can be achieved at higher S-ZVIN concentrations. The most probable reason for this phenomenon is related to the increase in the reactive sites of S-ZVIN surfaces by enhancing the concentration of S-ZVIN [45]. Similar results have been reported in previous studies [46,47].

4. Process Optimization of Cr(VI) Removal

The optimization procedure of Cr(VI) removal was carried out to optimize the experimental conditions and to achieve the maximum treatment performance. The optimal experimental conditions for Cr(VI) removal were obtained in solution pH of 4.70, S-ZVIN concentration of 1.30 g·L^{-1} and the reaction time of 75 min. Furthermore, an experiment was conducted with optimal conditions to confirm the results of optimization. Results showed that the obtained Cr(VI) removal efficiency of the experiment agreed well with the predicted value from the model that apparently verified the results obtained from RSM. Our findings revealed that RSM is a promising method for optimization of Cr(VI) removal efficiency from aqueous solution using S-ZVIN.

5. Kinetic Studies of Cr(VI) Removal

Figs. 6 and 7(a)-(c) illustrate the results of the kinetic studies of Cr(VI) removal utilizing different kinetic models. Clearly, all the applied models can describe the kinetic removal of Cr(VI) at different pH values of aqueous solutions and S-ZVIN concentrations. It is noteworthy that all kinetic experiments were performed in the reaction time of 90 min as equilibrium time obtained from preliminary experiments. The coefficients of determination (R^2) and other parameters of each kinetic model are presented in Tables 5 to 6. The larger R^2 value is, the more suitable the corresponding model will be. According to these tables, in the case of pseudo first-order and pseudo-second order kinetic models, the k_{obs} and k decreased by enhancing pH values. For pseudo zero-order model, however, a fluctuating trend was observed. The results from Shi et al. [48] for Cr(VI) removal using Bentonite-supported ZVIN revealed that increasing pH values from 4 to 8 caused a decrease in k_{obs} from 0.0275 to 0.0083 (min^{-1}) [48]. Besides, Wang et al. (2010) performed reductive removal of Cr(VI) using iron-encapsulated alginate beads and reported that the removal of Cr(VI) was absolutely pH-dependent [46]. At different S-ZVIN concentrations, pseudo first-order kinetic model could efficiently describe Cr (VI) removal (R_1^2>0.91). At different S-ZVIN concentrations of 0.5, 0.75, 1, 1.5 and 2 g·L^{-1}, the corresponding k_{obs} was 0.017, 0.0337, 0.0412, 0.0533 and 0.0573 (min^{-1}), respectively. Previous studies have shown that the pseudo first-order kinetic model strongly relies on the concentration of zero-valent iron nanoparticles [49]. Finally, in all experimental conditions, among the studied kinetic models, the pseudo first-order kinetic model with high R^2 could better describe the kinetic parameters of Cr(VI) compared to all other models.

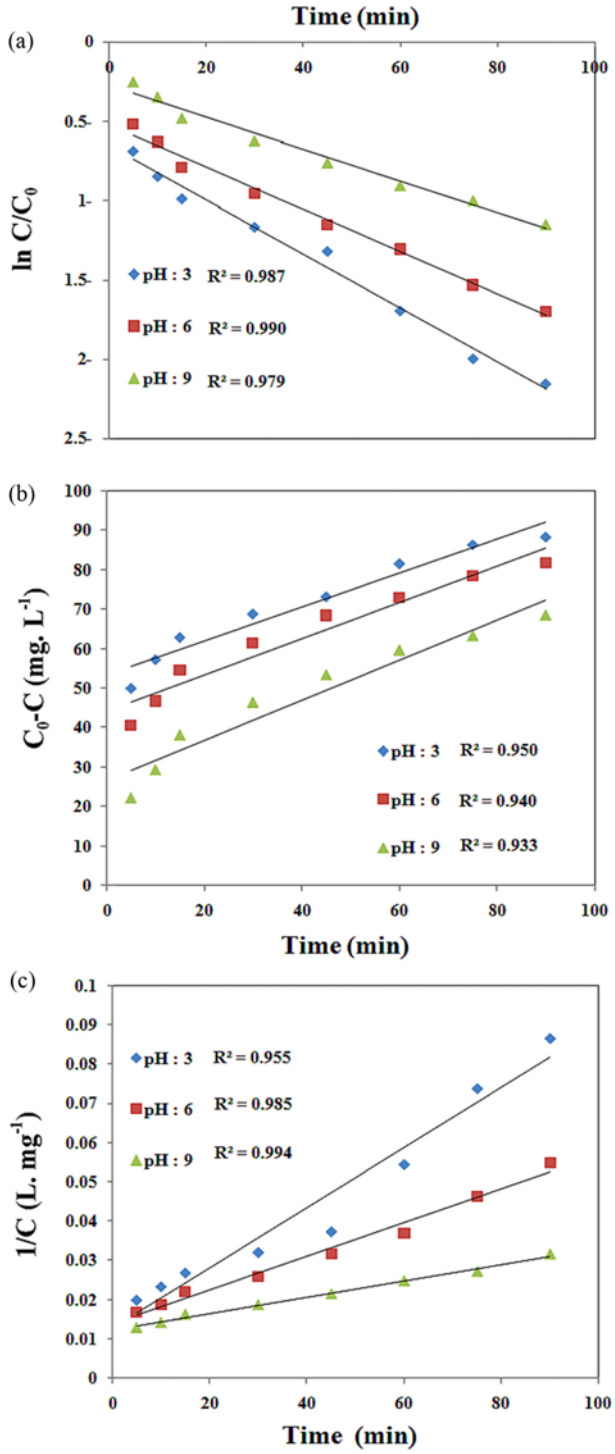

Fig. 6. Pseudo first-order (a), Zero-order (b) and pseudo second-order (c) kinetic studies of Cr(VI) removal at different pH values.

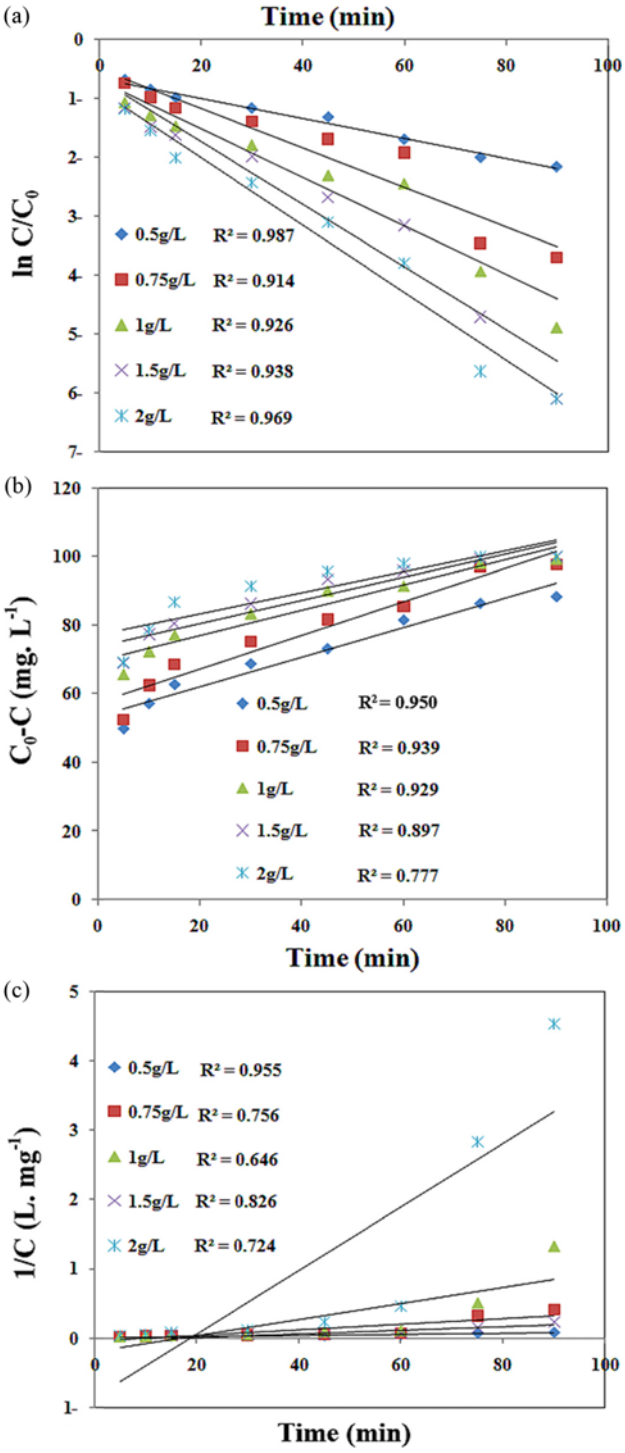

Fig. 7. Pseudo first-order (a), Zero-order (b) and pseudo second-order (c) kinetic studies of Cr(VI) removal at different S-ZVIN concentration.

Table 5. Kinetic parameters of Cr(VI) removal at different pH values

pH of aqueous solution	Pseudo zero-order kinetic model		Pseudo first-order kinetic model		Pseudo second-order kinetic model	
	k_{zero} (mg L^{-1} min^{-1})	R_0^2	k_{obs} (min^{-1})	R_1^2	k (min gmg^{-1})	R_2^2
3	0.4312	0.95	0.017	0.987	0.0008	0.955
6	0.4587	0.94	0.0134	0.99	0.0004	0.985
9	0.5065	0.933	0.01	0.979	0.0002	0.994

Table 6. Kinetic parameters of Cr (VI) removal at different concentrations of S-ZVIN

S-ZVIN concentration ($g \cdot L^{-1}$)	Pseudo zero-order kinetic model		Pseudo first-order kinetic model		Pseudo second-order kinetic model	
	k_{zero} ($mg\ L^{-1}\ min^{-1}$)	R_0^2	k_{obs} (min^{-1})	R_1^2	k ($min\ gmg^{-1}$)	R_2^2
0.5	0.4312	0.95	0.017	0.987	0.0008	0.955
0.75	0.4892	0.939	0.0337	0.914	0.0041	0.756
1	0.3703	0.929	0.0412	0.926	0.0115	0.646
1.5	0.3357	0.897	0.0533	0.938	0.0026	0.826
2	0.3077	0.777	0.0573	0.969	0.0457	0.724

CONCLUSIONS

The present study was conducted with the aim of Cr(VI) removal from aqueous solutions using sepiolite-stabilized ZVIN. The optimization process of Cr(VI) removal from aqueous solutions using S-ZVIN employed central composite design. In this regard, pH of the aqueous solution, the reaction time and the S-ZVIN concentration were selected as independent variables affecting Cr(VI) removal, and the removal efficiency of Cr(VI) was considered as a response. The results showed that all independent variables significantly influenced the Cr(VI) removal. Furthermore, the level of the experimental variables, 4.7 for initial pH of aqueous solution, 1.3 g L^{-1} for S-ZVIN dosage and 75 min for the reaction time, were obtained as optimum conditions for removal efficiency of Cr(VI). The removal rate for optimum condition was obtained to be 98.15%. Furthermore, results of kinetic studies demonstrated that a pseudo-first order kinetic model was the most suitable one compared to all other kinetic models in the study of Cr(VI) removal using S-ZVIN.

ACKNOWLEDGEMENT

The authors gratefully acknowledge Shahid Chamran University of Ahvaz and University of Tabriz, for all supports they provided for this study.

ABBREVIATIONS

ANOVA : analysis of variance
CCD : central composite design
Cr(VI) : hexavalent chromium
EDS : energy x-ray spectroscopy
OH^- : hydroxyl group
RSM : response surface methodology
SEM : scanning electron microscope
S-ZVIN : sepiolite-stabilized zero-valent iron nanoparticles
TEM : transmission electron microscope
ZVIN : zero-valent iron nanoparticles

REFERENCES

1. C. D. Palmer and R. W. Plus, EPA, 540/5-94/505 (1994).
2. World Health Organization, *Guidelines for drinking water quality, Health criteria and other supporting information*, WHO, Geneva, **2** (1996).
3. M. Pantsar-Kallio, S. P. Reinikainen and M. Oksanen, *Anal. Chim. Acta*, **439**, 9 (2011).
4. International Agency for Research on Cancer (IARC), *Chromium and chromium compounds*; IARC Monograph Evaluating Carcinogenic Risks to Humans, 49 (1990).
5. J. Cao and W. Zhang, *J. Hazard. Mater.*, **132**, 213 (2006).
6. I. Zongo, J. P. Leclerc, H. A. Maig, J. Wethe and F. Lapicque, *Sep. Purif. Technol.*, **66**, 159 (2009).
7. D. G. Kim, Y. H. Hwang, H. S. Shin and S. O. Ko, *Desal. Water Treat.*, **49**, 147 (2012).
8. L. Alidokht, A. R. Khataee, A. Reyhanitabar and S. Oustan, *Desalination*, **270**, 105 (2011).
9. D. I. Song, Y. H. Kim and W. S. Shin, *Korean J. Chem. Eng.*, **22**, 67 (2005).
10. A. Ramazanpour Esfahani, A. Farrokhian. Firouzi, G. Sayyad, A. Kiasat, L. Alidokht and A. R. Khataee, *Res. Che. Intm.*, **40**, 431 (2014).
11. F. W. Chuang, R. A. Larson and M. S. Wessman, *Environ. Sci. Technol.*, **29**, 2460 (1995).
12. C. M. Wai, H. K. Yak, B. W. Wenclawiak, I. F. Cheng and J. G. Doyle, *Environ. Sci. Technol.*, **33**, 1307 (1999).
13. A. Agrawal and P. G. Tratnyek, *Environ. Sci. Technol.*, **30**, 153 (2005).
14. J. Z. Badstra, R. Miehr, R. L. Johnson and P. G. Tratnyek, *Environ. Sci. Technol.*, **39**, 230 (2005).
15. T. Satapanajaru, P. Anurakpongsatorn, A. Songsasen, H. Boparai and J. Park, *Water. Air. Soil. Pollut.*, **175**, 361 (2006).
16. Y. P. Sun, X. Q. Li, W. X. Zhang and H. P. Wang, *J. Colloid Interface Sci.*, **308**, 60 (2007).
17. F. He and D. Zhao, *Environ. Sci. Technol.*, **39**, 3314 (2005).
18. H. Feng, M. Zhang, T. Qian and D. Zhao, *J. Colloid Interface Sci.*, **334**, 96 (2009).
19. Y. H. Lin, H. H. Tseng, M. Y. Wey and M. D. Lin, *Colloids Surf., A.*, **349**, 134 (2009).
20. A. Tiraferri, K. L. Chen, R. Sethi and M. Elimelech, *J. Colloid Interface Sci.*, **324**, 71(2008).
21. A. Reyhanitabar, L. Alidokht, A. R. Khataee and S. Oustan, *Eur. J. Soil. Sci.*, **63**, 724 (2012).
22. X. Zhang, S. Lin, Z. Chen, M. Megharaj and R. Naidu, *Water Res.*, **45**, 3481 (2011).
23. J. C. Sin, S. M. Lam and A. R. Mohamed, *Korean J. Chem. Eng.*, **28**, 84 (2011).
24. N. KeshavarzJafarzadeh, H. Sharifnia, S. N. Hosseini and F. Rahimpour, *Korean J. Chem. Eng.*, **28**, 531 (2011).
25. S. Murugesan, S. Rajiv and M. Thanapalan, *Korean J. Chem. Eng.*, **26**, 364 (2009).
26. S. B. Imandi, R. Chinthala, S. Saka, R. R. Vechalapu and K. K. Nalla, *Korean J. Chem. Eng.*, **30**, 1067 (2013).

27. D. Kim, Y. Song and Y. Park, *Korean J. Chem. Eng*., **30**, 664 (2013).
28. Y. Song, D. Kim and Y. Park, *Korean J. Chem. Eng*., **28**, 156 (2011).
29. S. Aber, A. R. Khataee and M. Sheydaei, *Bioresour. Technol*., **100**, 6586 (2009).
30. S. Ishak and A. Malakahmad, *Korean J. Chem. Eng*., **30**, 1083 (2013).
31. L. Alidokht, A. R. Khataee, A. Reyhanitabar and S. Oustan, *Clean-Soil. Air Water*, **39**, 633 (2011).
32. A. Murugesan, L. Raavikumar, V. SathyaSelvaBala, P. Senthikumar, T. Vidhyadevi, S. Dinesh Kirupha, S. S. Kalaivani, S. Krithiga and S. Sivanesan, *Desalination*, **271**, 199 (2011).
33. A. R. Khataee, *Environ. Technol*., **31**, 73 (2010).
34. A. Aleboyeh, N. Daneshvar and M. B. Kasiri, *Chem. Eng. Process*., **47**, 827 (2008).
35. P. D. Haaland, *Experimental design in biotechnology*, Marcel Dekker, New York, Basel (1989).
36. W. Yin, J. Wu, P. Li, X. Wang, N. Zhu, P. Wu and B. Yang, *Chem. Eng. J*., **181**, 198 (2010).
37. Y. Xu and D. Zhao, *Water. Res*., **41**, 2101 (2007).
38. S. Hojati and H. Khademi, *J. Cent. South. Univ. T*., **20**, 3627 (2013).
39. H. L. Liu and Y. R. Chiou, *Chem. Eng. J*., **112**, 173 (2005).
40. E. Cicek, C. Cojocaru, G. Zakrzewska-Trznadel, M. Harasimowicz and A. Miskiewicz, *Environ. Technol*., **33**, 51 (2012).
41. C. Zhang, Z. Zhu, H. Zhang and Z. Hu, *J. Environ. Sci*., **24**, 1021 (2012).
42. G. N. Jovanovic, P. ZnidarsicPlazl, P. Sakrittichai and K. Al-Khaldi, *Ind. Eng. Chem. Res*., **44**, 5099 (2005).
43. R. M. Powell, R. W. Puls, S. K. Hightower and D. A. Sabatini, *Environ. Sci. Technol*., **29**, 1913 (1995).
44. H. Zhou, Y. He, Y. Lan, J. Mao and S. Chen, *Chemosphere*, **72**, 870 (2008).
45. Z. Fang, X. Qiu, R. Huang, X. Qiu and M. Li, *Desalination*, **280**, 224 (2011).
46. M. J. Alowitz and M. M. Sherer, *Environ. Sci. Technol*., **36**, 299 (2002).
47. X. S. Wang, Y. J. Tang, L. F. Chen, F. Y. Li, W. Y. Wan and Y. B. Tan, *Clean-Soil. Air Water*, **38**, 236 (2010).
48. L. Shi, X. Zhang and Z. Che, *Water Res*., **45**, 886 (2011).
49. S. M. Ponder, J. G. Darab and T. E. Mallouk, *Environ. Sci. Technol*., **34**, 2564 (2000).